DOI: https://doi.org/10.62985/j.huit_ojs.vol24.no5.141

PERFORMANCE ANALYSIS OF ENERGY HARVESTING AND RECONFIGURABLE INTELLIGENT SURFACE AIDED COOPERATIVE COMMUNICATION OVER RAYLEIGH FADING CHANNEL

Duong Hien Thuan*, Nguyen Xuan Tien

Faculty of Electronics and Telecommunications, Saigon University

*Email: *thuan.duong@sgu.edu.vn*

Received: 19 June 2024; Accepted: 16 August 2024

ABSTRACT

In this research, we're employing Reconfigurable Intelligent Surfaces (RIS) and energy harvesting to figure out the cooperative communications throughput and outage probability in Rayleigh fading channel. The source harvests energy through the utilization of the Radio Frequency (RF) signal that the source receives from the Power Beacon (PB). Any node that emits a radio signal can serve as Node PB. The collected energy is used to transmit data to an intended recipient with the aided RIS. This work gives the closed expression of outage probability of the RIS-aided system with or without direct transmission link based on numerous system quality of service (QoS) requirements and investigates the impact of energy harvesting (EH) duration on the outage performance as well as exploits the Goden Section search method to optimize time splitting (TS) factor.

Keywords: Reconfigurable intelligent surfaces, Outage probability, Energy harvesting, Throughput.

1. INTRODUCTION

Reflecting Intelligent Surfaces (RIS) can be utilized to boost throughput in future wireless networks since all reflected signals can be controlled to achieve full diversity [1, 2]. The phase of channel gain between the source and the RIS, as well as the phase of channel gain between the RIS and the destination, are used to determine the phase shifts when using RIS as a reflector [3]. Another option is to use RIS as a transmission method [4]. The nth reflector's phase is optimized so that all reflections arrive at their destination with the same phase [5, 6] (reach full diversity). As a result, the receiver's output may be thought of as the Maximum Ratio Combiner's (MRC) output. IRS can provide a gain of 10-40 dB over traditional wireless systems without RIS over a range of reflector counts (K = 8, 16,...1024) [7]. In [8] and [9], a hardware implementation of RIS was covered. Non-Orthogonal Multiple Access (NOMA) systems that assign a set of dedicated reflectors to each user can employ RIS [10-13]. RIS has been proposed as a method of enhancing data rates for hybrid RF/FSO (Radio Frequency and Free Space Optical) communications, Multiple Input Multiple Output (MIMO) systems, and millimeter wave communications [14-17]. In [15], it was determined how well RIS with finite phase shifts performed for wireless communications. An analysis of the Max-Min SNR of multi-antenna wireless communications using IRS was carried out in [18]. The performance of the backscatter link and the direct link in RIS systems has been compared [19]. Unmanned Aerial Vehicles (UAV) have made use of RIS [20]. In [21], RIS employing machine learning methods was investigated. In [22], several wireless communication experimental outcomes

employing RIS were shown. In reference [23], a low complexity channel estimator for RIS has been proposed. In [24], studies on Orthogonal Multiple Access (OMA) and NOMA have been conducted using RIS. Additionally, RIS was proposed for two-way and Device to Device (D2D) communications [25, 26]. An investigation of the Quality of Service (QoS) of wireless communications through the use of intelligent reflecting surfaces was performed in [27]. A nonstationary channel model for wireless communications with intelligent reflecting surfaces was released in [28]. An approach was presented for millimeter wave communications with intelligent reflecting surfaces in [29]. In [30] sensor nodes and intelligent reflecting surfaces were used for the Internet of Things (IoT) network. Almost all investigations of RIS mentioned above do not apply energy harvesting (EH) techniques.

IoT devices rely on batteries for power. However, due to the limited lifetime of batteries, there is a significant need for self-powered devices or alternative energy sources to ensure continuous operation of IoT devices. Energy harvesting makes it possible to use RF signals, wind, or solar energy to extend the network's lifespan. Radiofrequency waves contain energy that can be retrieved in a direct proportion to the channel coefficient's squared absolute value. With energy harvesting systems, data can be sent from the source to the destination without the need for battery replacements or recharges.

Based on the benefits of RIS and EH approach, we exploit the use of EH in wireless cooperative communication with the aids of RIS in this paper with following principal contributions.

- We propose a RIS-aided cooperative communication, where the source harvests energy from RF received signals in faction of time duration and uses harvested energy to transmit the desired signal to destination. The closed-form expressions of system outage probability and throughput are derived in scenarios of RIS deployed as a reflector to transport signals in place of a conventional relay with and without direct transmission (DT) link.
- The simulation results validate the accuracy of the theoretical derivation findings. Furthermore, the simulation results show the impacts of various system parameters such as number of reflecting elements of RIS, Time splitting factor, target rate, transmit SNR.
- To investigate the impact of the time splitting factor on system's outage performance. The Golden Section search is used as an optimal solution of the time splitting factor to minimize the system's outage probability with various system scenarios.

Here is what's left in the paper: The system model and channel's characteristics are displayed and described in Section 2. The calculations based on outage probability and throughput are given in Section 3, the optimization of time spitting factor based on Goden Section searches are given in Section 4. The numerical analysis, together with simulations and in-depth discussions, is presented in Section 5. A brief summary of the study's contributions is given in Section 6.

2. SYSTEM MODEL AND CHANNEL CHARACTERISTICS

2.1. System model

We look at a wireless communication system, as shown in Fig. 1, where a signal is being transmitted from the source (S) to the destination (D). In the first fraction of time duration, the source harvests energy from RF wave which emitted from Power Beacon (PB). In the second fraction of time duration, the source uses harvested energy to transmit desired signal to destination in both ways which are direct link and via RIS as relay. The RIS consists of N reflectors (reflecting elements) and acts as passive reflecting surface.

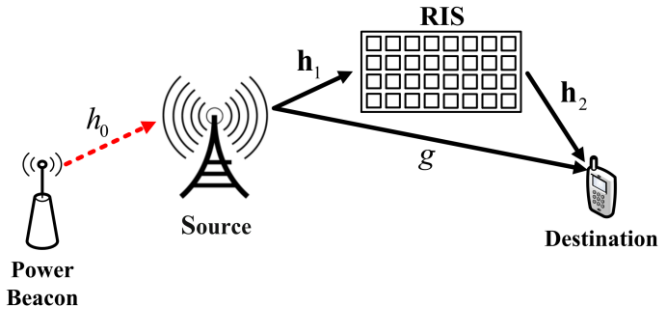

Fig.1. RIS-aided cooperative communication system

We assume that the source S collects energy for αT seconds, where T is the frame period and $0<\alpha<1$, α is called TS (Time Splitting) factor. The harvesting energy is based on the received RF signal from node PB. For the remaining portion of the frame, or $(1-\alpha)$T seconds, data is sent to the destination using the energy that S has captured. We compute the throughput in the case of different RIS configurations acting as reflectors. We also recommend that the harvesting period be optimized in order to enhance throughput. A short harvesting period results in little gathered energy and a poor throughput. There won't be enough time for data transmission for the rest of the frame, or $(1-\alpha)$T, if the harvesting length is long enough. S extracts energy from the RF signal that PB sends. The quantity of energy gathered is equivalent to

$$E=\eta\alpha TP_{PB}|h_0|^2 \tag{1}$$

where $0<\eta<1$ presents the energy conversion efficiency, P_{PB} is the power of node PB and h_0 is the channel coefficient between PB and S. The average power of channel coefficient h_0 is $\mathbb{E}\left\{|h_0|^2\right\}=\lambda_0$ where $\mathbb{E}\{X\}$ is the expectation of X.

As in several prior works, we assume that the information transmission uses all of the harvested energy. Thus, the source's transmit power is determined by

$$P_S=\frac{E}{(1-\alpha)T}=\frac{\eta\alpha P_{PB}}{(1-\alpha)}|h_0|^2 \tag{2}$$

S uses the gathered energy to transmit the separate signal to the destination via the RIS paradigm during the wireless information transfer (WIT) phase. Consequently, the signal that was received at the destination can be stated as

$$y=\left(\mathbf{h}_2^T\mathbf{\Phi}\mathbf{h}_1+g\right)\sqrt{P_S}x+z \tag{3}$$

where $(.)^T$ denotes the transpose operator, g indicates the direct link from S to D channel and x represents the normalized transmit signal with unit energy with $\mathbb{E}\left\{|x|^2\right\}=1$. The $N\times1$ vectors $\mathbf{h}_1$ and $\mathbf{h}_2$ symbolize the S-RIS and RIS-D channels, respectively. Also, the $N\times N$ matrix $\mathbf{\Phi}=\text{diag}\{\theta\}$ stands for the matrix of phase shifts, where $\theta=\left[e^{j\theta_1},e^{j\theta_2},\ldots,e^{j\theta_N}\right]$ with $\theta_n\in[0,2\pi)$ representing the phase shift of the n^{th} RIS reflecting element. Finally, the additive white Gaussian noise with zero mean and variance N_0 is represented by the symbol z.

For simplicity, Eq. (3) can be rewritten as

$$y = \left(\sum_{n=1}^{N} h_{1,n} e^{j\theta_n} h_{2,n} + g \right) \sqrt{P_S}\, x + z \tag{4}$$

And the receive SNR at destination can be given by

$$\bar{\gamma} = \frac{P_S}{N_0} \left| \sum_{n=1}^{N} h_{1,n} e^{j\theta_n} h_{2,n} + g \right|^2 \tag{5}$$

To maximize the achievable rate and minimize outage probability, the receive SNR Eq. (5) needs to be maximized by optimizing phase shifts. we consider the ideal phase shift matrix and perfect statistical channel state information (CSI) at the RIS, the optimal phase shift is given by [31], [32].

$$\theta_n = \angle \frac{g}{h_{1,n} h_{2,n}}, \quad n = 1, ..., N \tag{6}$$

where $h_{1,n}$ and $h_{2,n}$ are the n^{th} elements of vectors $\mathbf{h}_1$ and $\mathbf{h}_2$, respectively, and $\angle x$ indicates the phase of the complex number x. It is mean that the total phase shift of incidence wave ($h_{1,n}$), reflected wave ($h_{2,n}$) and the shift phase (θ_n) are equal to the phase of direct link (g). So the received power is improved due to coherent combining.

The maximum SNR of the system can be computed as [33]

$$\bar{\gamma}_{\max} = \frac{P_S}{N_0} \left(\sum_{n=1}^{N} \left| h_{1,n} \right| \left| h_{2,n} \right| + \left| g \right| \right)^2 \tag{7}$$

Submitting (2) into (7), $\gamma_{\max}$ is given by

$$\gamma_{\max} = \delta \left| h_0 \right|^2 \left| Q \right|^2 \tag{8}$$

where $\rho = \frac{P_{PB}}{N_0}$ represents the transmit SNR, $\delta = \frac{\eta \alpha \rho}{(1-\alpha)}$ and $Q = \sum_{n=1}^{N} \left| h_{1,n} \right| \left| h_{2,n} \right| + \left| g \right|$.

2.2. Channel characteristics

In this paper, we utilize a block-fading channel model in which each coherent interval's channels are quasi-static. Specifically, the channels between the transmitter and receiver is used in the uncorrelated Rayleigh channel model, for which the channel between PB and source is h_0; between source and destination is g; between source and n^{th}-element of IRS is $h_{1,n}$; between n^{th}-element of IRS and destination is $h_{2,n}$, respectively.

Furthermore, the RVs of $|\chi|$ with Rayleigh distributions and $|\chi|^2$ have exponential distributions [34] as below

$$f_{|\chi|^2}(x) = \frac{1}{\lambda_\chi} e^{-\frac{x}{\lambda_\chi}} \tag{9a}$$

$$F_{|\chi|^2}(x) = 1 - e^{-\frac{x}{\lambda_\chi}} \tag{9b}$$

where $\chi \in \{h_0, g, h_{1,n}, h_{2,n}\}$, $n = 1, 2, ..., N$, λ_χ is average power of channel χ.

In Eq. (8), maximized SNR is a function of channel coefficients, $|Q|^2$, therefore we need the CDF and PDF of $|Q|^2$ for evaluating system performance. For the optimizing phase shifts, the cumulative distribution function (CDF) of $|Q|^2$ can be obtained in [35] as

$$F_{|Q|^2}(x) = 1 - \frac{\mathbf{\Gamma}\left(k, \frac{\sqrt{x}}{\omega}\right)}{\mathbf{\Gamma}(k)} \tag{10}$$

where $\mathbf{\Gamma}(k)$ is the Gamma function, $\mathbf{\Gamma}(k, \omega)$ is the upper incomplete Gamma function, the shape parameter k and scale parameter ω are

$$k = \frac{\left(\sqrt{\pi\lambda_g} + 2N\xi\zeta\right)^2}{4\lambda_{g_i} + 4N\xi\zeta^2 - \pi\lambda_g} \tag{11a}$$

$$\omega = \frac{4\lambda_g + 4N\xi\zeta^2 - \pi\lambda_g}{2\left(\sqrt{\pi\lambda_g} + 2N\xi\zeta\right)} \tag{11b}$$

where $\xi = \pi^2 / \left(16 - \pi^2\right)$ and $\zeta = \left(4 - \pi^2/4\right)\sqrt{\lambda_{h_1}\lambda_{h_2}} / \pi$

With the aid Eq. (8.354.2) of [36], (10) can be derived as

$$F_{|Q|^2}(x) = \frac{1}{\mathbf{\Gamma}(k)} \sum_{q=0}^{\infty} \frac{(-1)^q x^{\frac{k+q}{2}}}{q!(k+q)w^{k+q}} \tag{12}$$

From (11), the expression for the probability density function (PDF) of $|Q|^2$ is as follows:

$$f_{|Q|^2} = \frac{\partial}{\partial x} F_{|Q|^2}(x) = \frac{1}{2\mathbf{\Gamma}(k)} \sum_{q=0}^{\infty} \frac{(-1)^q x^{\frac{k+q-2}{2}}}{q! w^{k+q}} \tag{13}$$

3. PERFORMANCE ANALYSIS

3.1. Outage probability

In general, the Quality of Service (QoS) can be considered as target rates at destination notes, system outage probability. Those QoS metrics are conceptually related to SNR which is thought to be a crucial statistic. The RIS-assisted wireless system's outage performance will be assessed in the next. Based on the definition of outage probability, the formula for outage probability of D can be written as

$$OP = \Pr\left(\gamma_{\max} < \gamma_{th}\right) \tag{14}$$

where the threshold SNR is $\gamma_{th} = 2^{\frac{2R}{1-\alpha}}$ where R is the desired rate at D.

From (8) into (14), OP can be written by

$$OP = \Pr\left(|Q|^2 < \frac{\gamma_{th}}{\delta |h_0|^2}\right) = \int_0^{\infty} f_{|h_0|^2}(x)\left[F_{|Q|^2}\left(\frac{\gamma_{th}}{\delta x}\right)\right]dx \tag{15}$$

Submitting (9a) and (12) into (15), the OP of D is calculated as

$$OP = \frac{1}{\lambda_0 \Gamma(k)} \sum_{q=0}^{\infty} \frac{(-1)^q}{q!(k+q) w^{k+q}} \left(\frac{\gamma_{th}}{\delta}\right)^{\frac{k+q}{2}} \int_0^{\infty} \frac{e^{-\frac{x}{\lambda_0}}}{x^{\frac{k+q}{2}}} dx. \tag{16}$$

With the additional assistance Eq. (3.351.3) of [36], the outage probability of D is given by

$$OP = \frac{\gamma_{th}^{\frac{k+q}{2}}}{\lambda_0^{\frac{k+q}{2}} \delta^{\frac{k+q}{2}} \Gamma(k)} \sum_{q=0}^{\infty} \frac{(-1)^q}{q!(k+q) w^{k+q}} \Gamma\left(-\frac{k+q}{2}+1\right) \tag{17}$$

3.2. Throughput analysis

Throughput in delay-limited transmission mode can be further assessed based on achievable outage probability as

$$\tau = (1 - OP) R. \tag{18}$$

4. QOS OPTIMIZATION WITH LINEAR ENERGY HARVESTING

From the analysis above, the system's outage performance has been determined using a linear energy harvesting model, which includes the outage probability and the outage throughput. In this case, we examine the QoS optimization strategies that are built upon outage performance. Ensuring system reliability, the minimization of outage probability scheme can fulfill QoS demands.

Equations (13)-(15) show a correlation between outage probability and time switching factor α. To optimize outage probability, determine the best solution for α, which may be represented as

$$\begin{aligned} \alpha^* &= \arg\min_{\alpha} OP \\ &s.t.\ 0 < \alpha < 1 \end{aligned} \tag{17}$$

where α^* denotes the optimal solution of α for minimizing the system outage probability. The answer to minimize (17) is unique and can be solved using a linear search strategy, such as the golden section approach. We solve the optimization problem using the Golden section approach, and the specific progress is presented in Algorithm 1.

Algorithm 1 Golden Section Search-Based Optimization Algorithm

Ensure: the optimal solution α^* for minimizing the system outage probability $OP(\alpha^*)$

1: **Input:** $GR = (\sqrt{5}-1)/2$, $a \leftarrow 0$, $b \leftarrow 1$, $\varepsilon \leftarrow 10^{-3}$

2: **Begin**

3: Calculate special middle points: $v_1 \leftarrow a + (b-a)*GR$ and $v_2 \leftarrow b - (b-a)*GR$

4: **while** $|b-a| \le \varepsilon$ **do**

5: Update: $OP_{\text{temp1}} = OP(v_1)$

6: Update: $OP_{\text{temp2}} = OP(v_2)$

7: **if** $OP_{\text{temp1}} < OP_{\text{temp2}}$ **then**

8: Update: $a \leftarrow v_2$ *% eliminate all value lesser than* v_2, v_2 *becomes new* a

9: **else**

10: Update: $b \leftarrow v_1$ *% eliminate all value greater than* v_1, v_1 *becomes new* b

11: **end**

12: Update: $v_1 = a + (b-a)*GR$

13: Update: $v_2 \leftarrow b - (b-a)*GR$

14: **end**

15: **return** optimal value of $\alpha^* = (b+a)/2$

16: **end**

where GR, ε are the Golden Ratio and maximum error tolerance, respectively; $a = 0$, $b = 1$ are the initial lower bound and upper bound of time splitting factor.

5. NUMERICAL RESULTS

In this part, we use Monte Carlo simulation to confirm the obtained outage probability. The primary parameters utilized are listed in Table 1, where BPCU denotes bit per channel and MATLAB software was used to execute the simulations.

Table 1. Parameters used in performance evaluation

Evaluating Parameters	Values
Repeated Monte Carlo Simulations	10^7 iterations
The target rate at D	$R = 2$ (BPCU)
The efficiency of energy conversion	h = 1
Time splitting factor	a = *0.5*
Total reflecting elements	*N = 4, 8, 16*
Channel power gains $\chi \in \{h_0, g, h_{1,n}, h_{2,n}\}$, $n = 1, 2, ..., N$	$\lambda_\chi = 1$

In Fig.2, the OP cures versus ρ for EH RIS-aided systems with and without DT link (scenarios of some obstructions that source could not directly transmit to destination) are

plotted. The likelihood of an outage diminishes as ρ increases. Additionally, the outage probability tends to decrease with large values of the number of RIS reflecting elements *N*. When number of RIS-elements is small, the impact of DT link is significant. For example, the system with DT link's performance is about 3dB better than the system without DT link's performance at the same outage probability. However, when *N* has a large value, the influence of DT link is no longer significant. For example, *N = 16*, the performance of the system with and without DT is almost the same.

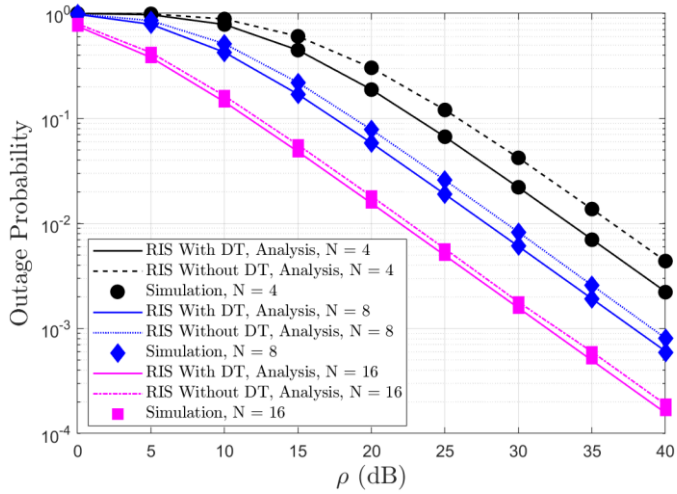

Fig.2. Outage Probability versus r for EH system with and without DT

In Fig. 3, we examine the likelihood of an outage in relation to the desired data rates with fixed transmit SNR (ρ = 20 dB). The number of RIS-reflecting elements is high, and the likelihood of an outage probability is trending downward. The contribution of RIS numbers to the system's outage probability is depicted in Fig.3. In this situation, the DT link has a powerful effect on the system performance.

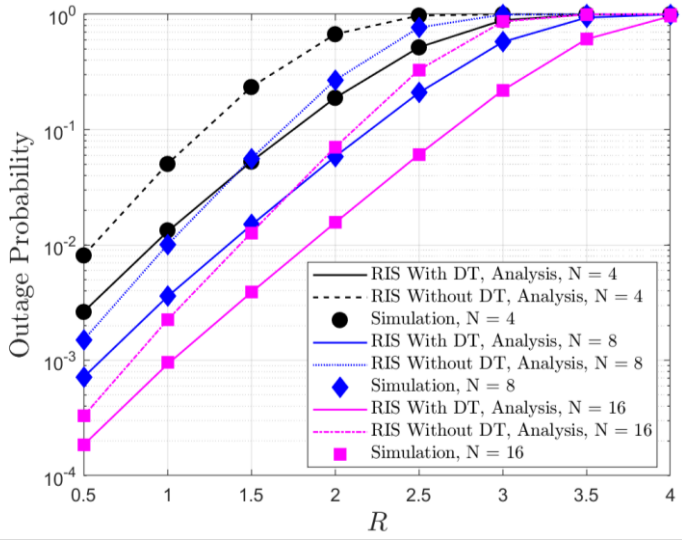

Fig.3. Outage probability of the destination versus R, with ρ = 20 dB

The outcome shown in Fig. 4 verifies that, in terms of the energy harvesting goal, there is an optimal value of the fraction the block time (TS factor) that minimize the system' outage probability. In the Fig.4, optimal TS factor can be estimated around 0.2605 for the number of

RIS elements N = 4, 8, 16. For calculating optimal TS factor, the Golden section search algorithms 1 in section 4 can be applied.

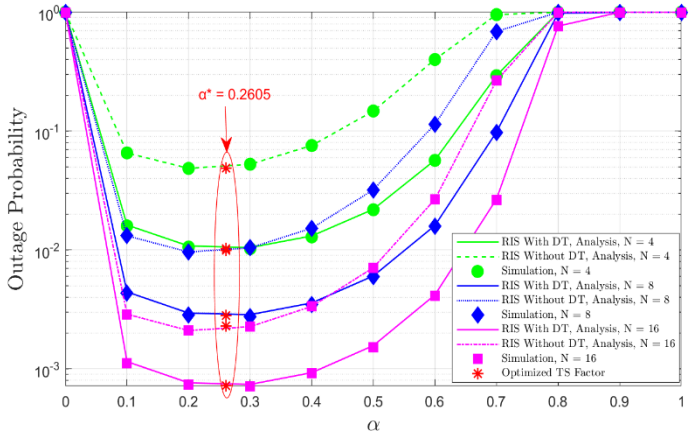

Fig.4. Outage probability of the destination versus α, with ρ = 30 dB

Fig.5 shows the OP cures versus ρ with $N = 16$ and different TS factor. As discuss in Fig.4, the optimal value of a for this case is about 0.2605. It is proved in the Fig.5 that the system performance with optimal a = 0.2605 is better than those of the system with TS factor of a = 0.1 and a = 0.5. With the optimization algorithm we can obtain the optimal TS factor to minimize the system outage probability.

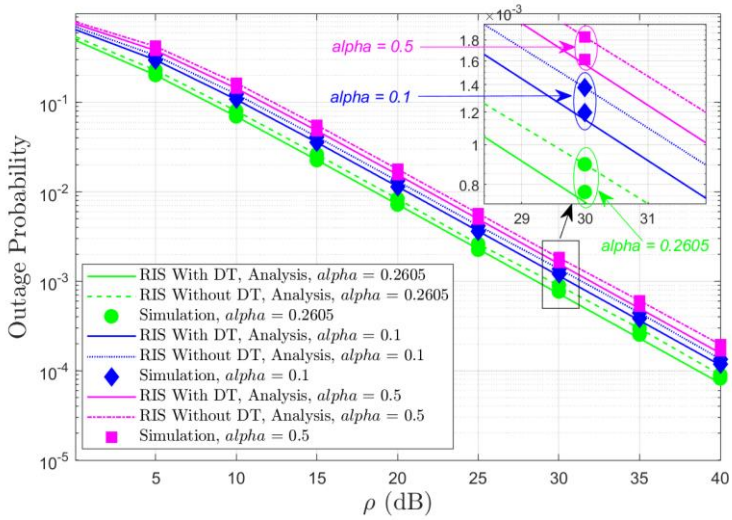

Fig.5. Outage Probability versus r with different TS factor

Finally, we can observe in Fig.6 that the simulated curves of throughput increase when the number of RIS-reflecting elements increases within mid-range of transmit SNR. In the low-range transmit SNR the throughput is very poor and nearly the same for the system with or without DT link as well as different number of reflecting-elements (N). And in the high-range transmit SNR, the throughput reaches the target and it is not affected of the DT link or number of reflecting-elements (N). However, in the mid-range of transmit SNR, the DT link as well as the number of RIS-elements are significantly impacting on system performance.

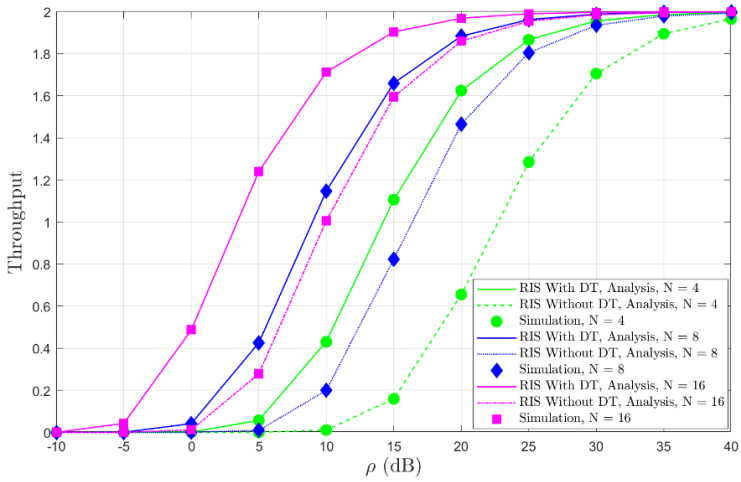

Fig.6. Throughput performance of the destination versus ρ

6. CONCLUSION

In this research, we calculated the throughput and outage probability of wireless cooperative communication where a RIS is used as relay and the source employs energy harvesting. An RF signal from another node PB is received by the source and provides the source with energy. Data is transmitted to destination by using the energy that has been gathered. We computed the throughput versus transmit SNR for a single RIS utilized as a reflector. Based on the TS protocol, this study produced an expression for the RIS-aided system's outage probability and calculated the system's throughput and outage probability of the proposed model, RIS-Aided system with or without DT link. This work gave the optimizing algorithm for the best solution of the TS factor that reduces outage probability in order to maximize system performance. The theoretical derivation and optimal solution were supported by the simulation results, which also showed how different system settings affect outage performance. The RIS-aided system with DT link exhibited better outage probability and throughput compares to RIS-aided system without DT link. The simulation also revealed that changing number reflectors (N) as well as the TS factor selections made a significant influence on system's outage performance.

Acknowledgment: This work is a part of the basic science research program CSB2023-09 funded by Saigon University.

REFERENCES

1. Peng Xu, Gaojie Chen, Zheng Yang, and Marco Di Renzo - Reconfigurable intelligent surfaces-assisted communications with discrete phase shifts: How many quantization levels are required to achieve full diversity? IEEE Wireless Communications Letters **10** (2) (2020) 358-362. https://doi.org/10.1109/LWC.2020.3031084
2. Le Chi-Bao, Do Dinh-Thuan, Li Xingwang, Huang Yung-Fa, Chen Hsing-Chung, Voznak Miroslav - Enabling NOMA in backscatter reconfigurable intelligent surfaces-aided systems. IEEE Access **9** (2021) 33782-33795. https://doi.org/10.1109/ACCESS.2021.3061429
3. Xianfu Lei, Mingjiang Wu, Fuhui Zhou, Xiaohu Tang, Rose Qingyang Hu, and Pingzhi Fan - Reconfigurable intelligent surface-based symbiotic radio for 6G: Design, challenges, and opportunities. IEEE Wireless Communications **28** (5) (2021) 210-216. https://doi.org/10.1109/MWC.121.2100126.

4. Ertugrul Basar - Reconfigurable intelligent surface-based index modulation: A new beyond MIMO paradigm for 6G. IEEE Transactions on Communications **68** (5) (2020) 3187-3196. https://doi.org/10.1109/TCOMM.2020.2971486
5. Qingqing Wu, and Rui Zhang - Towards smart and reconfigurable environment: Intelligent reflecting surface aided wireless network. IEEE communications magazine **58** (1) (2019) 106-112. https://doi.org/10.1109/MCOM.001.1900107
6. Nhan Duc Nguyen, Chi-Bao Le, and Munyaradzi Munochiveyi - Uplink multiple access for reconfigurable intelligent surface-aided wireless systems. Wireless Communications and Mobile Computing **2022** (1) 1932708. https://doi.org/10.1155/2022/1932708
7. Chongwen Huang, Alessio Zappone, George C. Alexandropoulos, Mérouane Debbah, and Chau Yuen - Reconfigurable intelligent surfaces for energy efficiency in wireless communication. IEEE Transactions on Wireless Communications **18** (8) (2019) 4157-4170. https://doi.org/10.1109/TWC.2019.2922609
8. Ruyu Luo, Wanli Ni, Hui Tian, and Julian Cheng - Federated deep reinforcement learning for RIS-assisted indoor multi-robot communication systems. IEEE Transactions on Vehicular Technology **71** (11) (2022) 12321-12326. https://doi.org/10.1109/TVT.2022.3190557.
9. Jintao Wang, Shiqi Gong, Qingqing Wu, and Shaodan Ma - RIS-aided MIMO systems with hardware impairments: Robust beamforming design and analysis. IEEE Transactions on Wireless Communications 2023. https://doi.org/10.1109/TWC.2023.3246990
10. Thirumavalavan V.C., Jayaraman T.S. - BER analysis of reconfigurable intelligent surface assisted downlink power domain NOMA system. In 2020 International Conference on COMmunication systems & NETworkS (COMSNETS), Bengaluru, India (2020) 519-522. https://doi.org/10.1109/COMSNETS48256.2020.9027303
11. Anh-Tu Le, Tran Dinh Hieu, Tan N. Nguyen, and Thanh-Lanh Le - Physical layer security analysis for RIS-aided NOMA systems with non-colluding eavesdroppers. Computer Communications **219** (2024) 194-203. https://doi.org/10.1016/j.comcom.2024.03.011
12. Anh-Tu Le, Tan N. Nguyen, Lam-Thanh Tu, Tin-Phu Tran, Tran Trung Duy, Miroslav Voznak, and Zhiguo Ding - Performance analysis of RIS-assisted ambient backscatter communication systems. IEEE Wireless Communications Letters **13** (3) (2024) 791-795. https://doi.org/10.1109/LWC.2023.3344113
13. Tan N. Nguyen, Nguyen Van Vinh, Ba Ca Nguyen, and Bui Vu Minh - On performance of RIS-aided bidirectional full-duplex systems with combining of imperfect conditions. Wireless Networks **30** (2) (2024) 649-660. https://doi.org/10.1007/s11276-023-03490-7
14. Hehao Niu, Zheng Chu, Fuhui Zhou, Cunhua Pan, Derrick Wing Kwan Ng, and Huan X. Nguyen - Double intelligent reflecting surface-assisted multi-user MIMO mmwave systems with hybrid precoding. IEEE Transactions on Vehicular Technology **71** (2) (2021) 1575-1587 DOI: https://doi.org/10.1109/TVT.2021.3131514.
15. Sung Hyuck Hong, Jaeyong Park, Sung-Jin Kim, and Junil Choi - Hybrid beamforming for intelligent reflecting surface aided millimeter wave MIMO systems. IEEE Transactions on Wireless Communications **21** (9) (2022) 7343-7357. https://doi.org/10.1109/TWC.2022.3157880.
16. Aman Sikri, Aashish Mathur, Prakriti Saxena, Manav R. Bhatnagar, and Georges Kaddoum - Reconfigurable intelligent surface for mixed FSO-RF systems with co-channel interference. IEEE Communications Letters **25** (5) (2021) 1605-1609. https://doi.org/10.1109/LCOMM.2021.3057116.

17. Boya Di, Hongliang Zhang, Lianlin Li, Lingyang Song ,Yonghui Li, and Zhu Han - Practical hybrid beamforming with finite-resolution phase shifters for reconfigurable intelligent surface based multi-user communications. IEEE Transactions on Vehicular Technology **69** (4) (2020) 4565-4570. https://doi.org/10.1109/TVT.2020.2973202.
18. Hui Gao, Kai Cui, Chongwen Huang, and Chau Yuen - Robust beamforming for RIS-assisted wireless communications with discrete phase shifts. IEEE Wireless Communications Letters **10** (12) (2021) 2619-2623. https://doi.org/10.1109/LWC.2021.3107319.
19. Qurrat-Ul-Ain Nadeem, Abla Kammoun, Aanas Chaaban, Mérouane Debbah, and Mohamed-Slim Alouini - Asymptotic max-min SINR analysis of reconfigurable intelligent surface assisted MISO systems. IEEE Transactions on Wireless Communications **19** (12) (2020) 7748-7764. https://doi.org/10.1109/TWC.2020.2986438.
20. Wenjing Zhao, Gongpu Wang, Saman Atapattu, Theodoros A. Tsiftsis, and Chintha Tellambura - Is backscatter link stronger than direct link in reconfigurable intelligent surface-assisted system? IEEE Communications Letters **24** (6) (2020) 1342-1346. https://doi.org/10.1109/LCOMM.2020.2980510.
21. Shenghai Chen, Liang Yang, Qi Zhu, Yongjie Yuan, Imran Shafique Ansari, and Guofu Zhu - On the performance of the UAV RIS-assisted dual-hop PLC-RF systems. IEEE Transactions on Vehicular Technology **72** (8) (2023) 11035-11040. https://doi.org/10.1109/TVT.2023.3261559.
22. Sheng Hua, and Yuanming Shi - Reconfigurable intelligent surface for green edge inference in machine learning. In 2019 IEEE globecom workshops (GC Wkshps), Waikoloa, HI, USA, 2019, pp. 1-6. https://doi.org/10.1109/GCWkshps45667.2019.9024398.
23. Linglong Dai, Bichai Wang, Min Wang, Xue Yang, Jingbo Tan, Shuangkaisheng Bi, Shenheng Xu, Fan Yang, Zhi Chen, Marco Di Renzo, Chan-Byoung Chae, and Lajos Hanzo - Reconfigurable intelligent surface-based wireless communications: Antenna design, prototyping, and experimental results. IEEE Access **8** (2020) 45913-45923. https://doi.org/10.1109/ACCESS.2020.2977772.
24. Na Li, Meng Li, Yuanwei Liu, Chaoying Yuan, Xiaofeng Tao - Intelligent reflecting surface assisted NOMA with heterogeneous internal secrecy requirements. IEEE Wireless Communications Letters **10** (5) (2021) 1103-1107. https://doi.org/10.1109/LWC.2021.3058768.
25. Xingwang Li, Yike Zheng, Ming Zeng, Yingting Liu, and Octavia A. Dobre - Enhancing secrecy performance for STAR-RIS NOMA networks. IEEE Transactions on Vehicular Technology **72** (2) (2022) 2684-2688. https://doi.org/10.1109/TVT.2022.3213334.
26. Sun Mao, Xiaoli Chu, Qingqing Wu, Lei Liu, and Jie Feng - Intelligent reflecting surface enhanced D2D cooperative computing. IEEE Wireless Communications Letters **10** (7) (2021) 1419-1423. https://doi.org/10.1109/LWC.2021.3069095.
27. Juanjuan Ren, Xianfu Lei, Zhangjie Peng, Xiaohu Tang, and Octavia A. Dobre - RIS-assisted cooperative NOMA with SWIPT. IEEE Wireless Communications Letters **12** (3) (2023) 446-450. https://doi.org/10.1109/LWC.2022.3229843.
28. Yuto Kawai, and Shinya Sugiura - QoS-constrained optimization of intelligent reflecting surface aided secure energy-efficient transmission. IEEE Transactions on Vehicular Technology **70** (5) (2021) 5137-5142. https://doi.org/10.1109/TVT.2021.3075685.
29. Yingzhuo Sun, Cheng-Xiang Wang, Jie Huang, and Jun Wang - A 3D non-stationary channel model for 6G wireless systems employing intelligent reflecting surfaces with practical phase shifts. IEEE Transactions on Cognitive Communications and Networking **7** (2) (2021) 496-510. https://doi.org/10.1109/TCCN.2021.3075438

30. Hongyang Du, Jiayi Zhang, Julian Cheng, Bo Ai - Millimeter wave communications with reconfigurable intelligent surfaces: Performance analysis and optimization. IEEE Transactions on Communications **69** (4) (2021) 2752-2768. https://doi.org/10.1109/TCOMM.2021.3051682.
31. Jiabao Gao, Caijun Zhong, Xiaoming Chen, Hai Lin, and Zhaoyang Zhang - Unsupervised learning for passive beamforming. IEEE Communications Letters **24** (5) (2020) 1052-1056. https://doi.org/10.1109/LCOMM.2020.2965532.
32. Qingqing Wu, Trung Q. Duong, Derrick Wing Kwan Ng, Robert Schober, and Rui Zhang - Intelligent Surfaces Empowered 6G Wireless Network, 2023: John Wiley & Sons, ISBN: 978-1-119-91312-2.
33. Qin Tao, Junwei Wang, and Caijun Zhong - Performance analysis of intelligent reflecting surface aided communication systems. IEEE Communications Letters **24** (11) (2020) 2464-2468. https://doi.org/10.1109/LCOMM.2020.3011843.
34. Dinh-Thuan Do, Chi-Bao Le, Alireza Vahid, and Shahid Mumtaz - Antenna selection and device grouping for spectrum-efficient UAV-assisted IoT systems. IEEE Internet of Things Journal **10** (9) (2023) 8014-8030. https://doi.org/10.1109/JIOT.2022.3229592.
35. Trinh Van Chien, Lam Thanh Tu, Symeon Chatzinotas, and Björn Ottersten - Coverage probability and ergodic capacity of intelligent reflecting surface-enhanced communication systems. IEEE Communications Letters **25** (1) (2020) 69-73. https://doi.org/10.1109/LCOMM.2020.3023759.
36. Gradshteyn, I.S. and I.M. Ryzhik - Table of integrals, series, and products. 7th Edition, Elsevier Academic Press, 2007.

TÓM TẮT

PHÂN TÍCH HIỆU NĂNG VỚI KỸ THUẬT THU NĂNG LƯỢNG CHO TRUYỀN THÔNG HỢP TÁC CÓ SỰ HỖ TRỢ MẶT PHẢN XẠ THÔNG MINH QUA KÊNH VÔ TUYẾN RAYLEIGH

Dương Hiển Thuận*, Nguyễn Xuân Tiên

Khoa Điện tử Viễn thông, Trường Đại học Sài Gòn

*Email: *thuan.duong@sgu.edu.vn*

Trong nghiên cứu này, bề mặt thông minh có thể cấu hình lại (RIS) được áp dụng cùng với kỹ thuật thu năng lượng để tính toán thông lượng truyền thông và xác suất dừng cho hệ thống truyền thông hợp tác qua kênh truyền fading Rayleigh. Năng lượng thu được thông qua việc sử dụng tín hiệu tần số vô tuyến (RF) từ Power Beacon (PB). Bất kỳ trạm nào phát ra tín hiệu vô tuyến đều có thể đóng vai trò là trạm PB. Năng lượng thu được sử dụng để truyền dữ liệu đến người nhận với sự hỗ trợ của RIS. Nghiên cứu này đưa ra biểu thức tính toán về xác suất dừng của hệ thống được hỗ trợ RIS có hoặc không có liên kết truyền trực tiếp từ nguồn đến đích dựa trên một số thông số về chất lượng dịch vụ (QoS) của hệ thống. Nghiên cứu này cũng xét đến tác động của hệ số phân chia khoảng thời gian thực hiện thu năng lượng (EH) dựa trên xác suất dừng của hệ thống và sử dụng thuật toán tối ưu dựa trên phương pháp tìm kiếm Golden để tìm ra hệ số phân chia thời gian tối ưu với xác suất dừng là cực tiểu.

Từ khóa: Bề mặt thông minh có thể cấu hình lại (RIS), xác suất dừng, thu năng lượng, thông lượng.